AGU PUBLICATIONS

Geophysical Research Letters

RESEARCH LETTER
10.1002/2015GL067009

Key Points:
- Seasonal forecasts of E_0 often have higher skill than do precipitation forecasts
- Greatest E_0 forecast skill is found in agricultural regions of the U.S. during the growing season
- Major improvements found when forecasts are initialized during moderate and strong ENSO

Supporting Information:
- Text S1 and S2, Figures S1–S6, Table S1, and Equation (S1)
- Figure S1
- Figure S2
- Figure S3
- Figure S4
- Figure S5
- Figure S6

Correspondence to:
D. J. McEvoy,
mcevoyd@dri.edu

Citation:
McEvoy, D. J., J. L. Huntington, J. F. Mejia, and M. T. Hobbins (2016), Improved seasonal drought forecasts using reference evapotranspiration anomalies, *Geophys. Res. Lett., 43*, 377–385, doi:10.1002/2015GL067009.

Received 12 NOV 2015
Accepted 17 NOV 2015
Accepted article online 24 NOV 2015
Published online 14 JAN 2016

Improved seasonal drought forecasts using reference evapotranspiration anomalies

Daniel J. McEvoy[1,2], Justin L. Huntington[1,2], John F. Mejia[1], and Michael T. Hobbins[3,4]

[1]Desert Research Institute, Reno, Nevada, USA, [2]Western Regional Climate Center, Reno, Nevada, USA, [3]Cooperative Institute for Research in Environmental Sciences, Boulder, Colorado, USA, [4]NOAA Earth System Research Laboratory, Physical Sciences Division, Boulder, Colorado, USA

Abstract A novel contiguous United States (CONUS) wide evaluation of reference evapotranspiration (ET_0; a formulation of evaporative demand) anomalies is performed using the Climate Forecast System version 2 (CFSv2) reforecast data for 1982–2009. This evaluation was motivated by recent research showing ET_0 anomalies can accurately represent drought through exploitation of the complementary relationship between actual evapotranspiration and ET_0. Moderate forecast skill of ET_0 was found up to leads of 5 months and was consistently better than precipitation skill over most of CONUS. Forecasts of ET_0 during drought events revealed high categorical skill for notable warm-season droughts of 1988 and 1999 in the central and northeast CONUS, with precipitation skill being much lower or absent. Increased ET_0 skill was found in several climate regions when CFSv2 forecasts were initialized during moderate-to-strong El Niño–Southern Oscillation events. Our findings suggest that ET_0 anomaly forecasts can improve and complement existing seasonal drought forecasts.

1. Introduction

A growing literature indicates that current dynamical seasonal precipitation (*Prcp*) forecasts contain limited skill past a 1 month lead time [e.g., *Lavers et al*., 2009; *Yuan et al*., 2011; *Yuan et al*., 2013; *Saha et al*., 2014; *Wood et al*., 2015]. Therefore, incorporating new drought-related variables with higher skill could add value and confidence to operational seasonal drought forecasts. Our understanding of drought dynamics and variability has evolved substantially over the last decade as evapotranspiration (ET) and physically based evaporative demand (reference ET (ET_0)) [*Allen et al*., 2005] has been shown to couple the land surface and atmosphere and so can be used in drought indicators [e.g., *Yao et al*., 2010; *Anderson et al*., 2011; *Mu et al*., 2013; *Otkin et al*., 2013; *Shukla et al*., 2015; *McEvoy*, 2015]. Anomalously high ET_0 is one of the contributing factors to intensification of extreme drought events, such as the 2012 to the present California drought [*Shukla et al*., 2015; *Williams et al*., 2015].

Research on seasonal ET_0 forecasts are limited to *Tian et al*. [2014], who evaluated bias-corrected maximum and minimum temperature (T_{max} and T_{min}, respectively), wind speed (U_z), downwelling shortwave radiation (R_d), and ET_0 over the southeast contiguous United States (CONUS). *Tian et al*. [2014] found Climate Forecast System version 2 (CFSv2) [*Saha et al*., 2014] ET_0 forecasts to have moderate skill during the cold season with the greatest skill when forecasts were initialized during El Niño–Southern Oscillation (ENSO) events (El Niño or La Niña conditions existed) and no skill during the warm season due to the inability of CFSv2 to fully resolve summer convection. An extensive CONUS wide skill analysis of CFSv2 ET_0, its drivers, and seasonal drought forecasting is absent from the literature and is the focus of this letter.

As an example of Prcp and ET_0 anomalies during drought, Figure 1 illustrates ET_0 (Figure 1a) and Prcp (Figure 1b) anomaly percentiles (with respect to a base period of 1982–2009) using gridded METDATA [*Abatzoglou*, 2011], for AMJ of 2002 period, one of the most severe droughts in the recorded history of the southwest [e.g., *Weiss et al*., 2009 and references therein]. Both ET_0 and Prcp anomalies identify similar magnitude and spatial patterns of wet (northwest MT and the Great Lakes) and dry regions (the southwest and the mid-Atlantic coast) and clearly demonstrate that ET_0 can successfully identify drought patterns (further comparison presented in Figure S1 in the supporting information). This occurs through (1) regional atmospheric dynamics that increase surface irradiance (through decreased cloudiness) and the vapor pressure deficit (through increased air temperature (T_{air}) and decreased humidity) and (2) local land surface-atmosphere feedbacks that lead to a complementary relationship between ET_0 and actual ET (a proxy for Prcp) under water limitations [*Hobbins and Huntington*, 2016; *McEvoy*, 2015]. In this letter, anomalies in ET_0

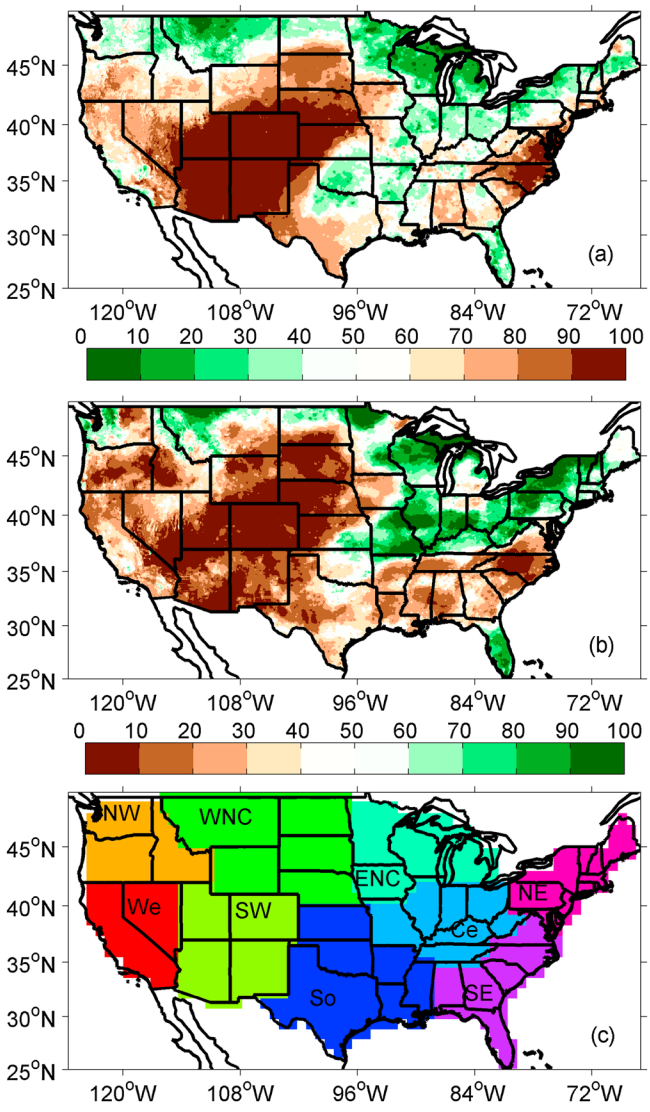

Figure 1. Accumulated (a) ET_0 and (b) Prcp anomaly percentiles from METDATA for AMJ 2002. Note that upper ET_0 and lower Prcp percentiles indicate drought (brown shading). (c) NCDC climate regions (described in section 2) on the CFSRF 1° grid used as area averaging domains for section 3 results. Regions are named as follows: northwest (NW), west (We), southwest (SW), west north central (WNC), south (So), east north central (ENC), central (Ce), southeast (SE), and northeast (NE).

derived from CFSv2 reforecasts (CFSRF) are evaluated over CONUS against METDATA in order to determine (1) if forecasts of ET_0 anomalies and its driving variables are skillful and in what regions and (2) if ET_0 anomalies can be forecast with greater skill than Prcp anomalies during droughts.

2. Data and Methodology

Nine-month continuous reforecasts from CFSv2 were obtained from NCEP, covering the retrospective period of 1982–2009. A detailed description of CFSRF can be found in *Saha et al.* [2014], and several other papers have presented CFSRF data distribution format [e.g., *Yuan et al.*, 2011; *Dirmeyer*, 2013]. Monthly ensembles (mean of forecasts initialized within the same month and year only) were created from CFSRF leads of 1–9 months, resulting in a range of 20 to 28 ensemble members per month (Table S1). This allows us to identify the impact of initialization month on forecast skill. To evaluate CFSRF skill, we use METDATA for 1982–2009. METDATA is a bias-corrected and spatially disaggregated (from 12 km to 4 km) product that combines the Parameter Regression on Independent Slopes Model [*Daly et al.*, 1994] with the North American Land Data Assimilation System version 2 [*Mitchell et al.*, 2004]. To test the sensitivity of observations to forecast skill, two other gridded data sets were also considered—the Climate Forecast System Reanalysis and the Modern Era Retrospective-analysis for Research and Applications—but differences in results as compared to using METDATA were negligible (not shown). To match the CFSRF spatial resolution, METDATA was averaged from daily to monthly values and resampled from 4 km to 1° using a bilinear interpolation. The following monthly variables were evaluated at 1° spatial resolution: Prcp, T_{max} (at 2 m), T_{min} (at 2 m), q (at 2 m), U_z (at 10 m), and R_d.

Following recommendations of *Allen et al.* [2005, equation 1], ET_0 was computed with the American Society of Civil Engineers Standardized Penman-Monteith equation using monthly METDATA and CFSRF. A priori, it is generally assumed that if the necessary data are available, ET_0 should be used over a T_{air}- and/or radiation-based method [*Hobbins et al.*, 2008; *Allen et al.*, 2005]. *Hobbins* [2016] demonstrated that the dominant drivers of ET_0 vary across CONUS depending on factors such as aggregation period (monthly versus annual) and season, and T_{air} is not always the dominant driver.

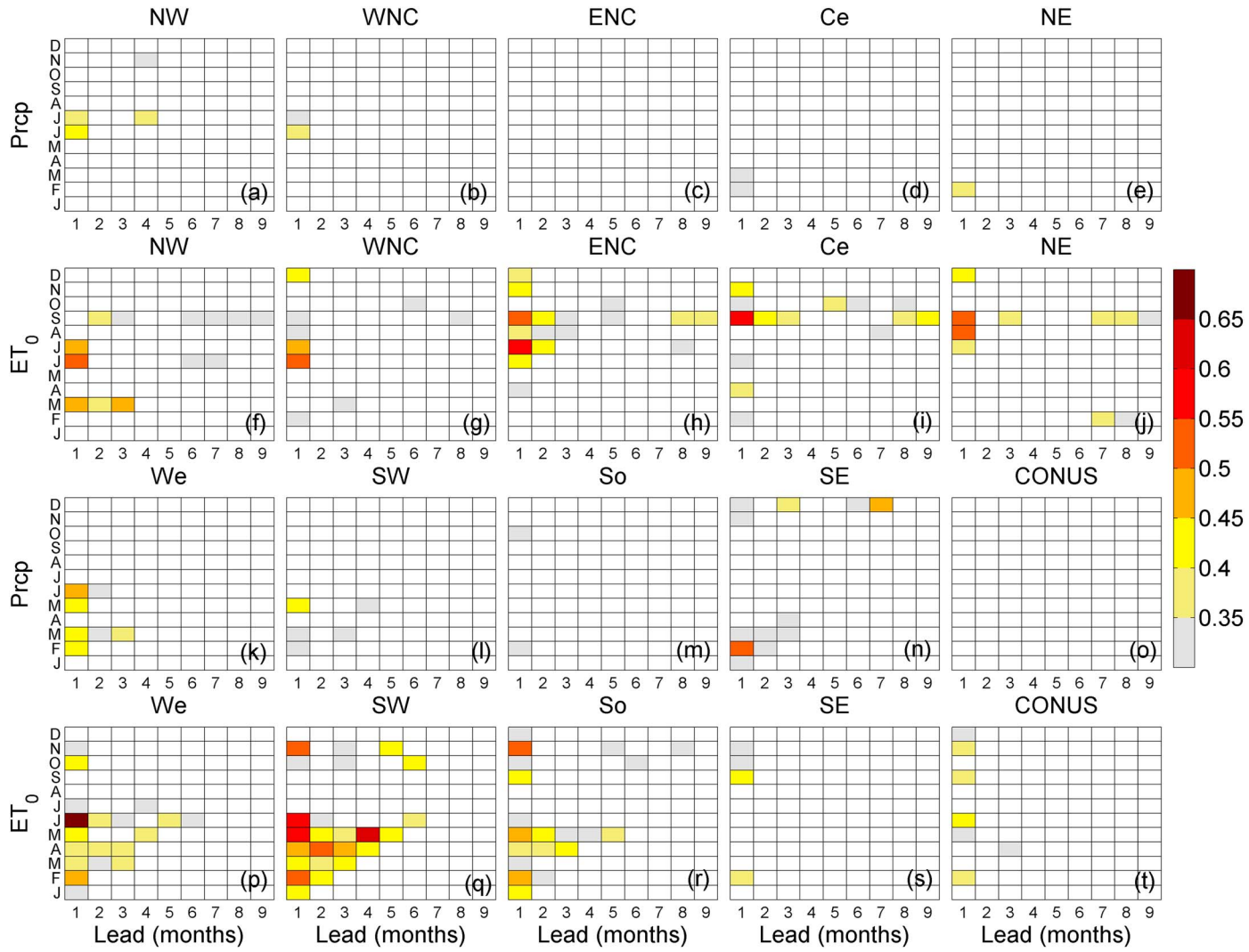

Figure 2. (f–j and p–t) Average ET_0 and (a–e and k–o) Prcp anomaly correlation (AC) between METDATA and CFSRF over each region (refer to Figure 1c for full region names and locations). Labels on the *x* axis indicate lead time (months) and labels on the *y* axis indicate the month for which the forecast is made. White boxes indicate AC < 0.3, which corresponds to $p > 0.06$ using a one-tailed probability.

The CONUS wide skill analysis of ET_0 and its drivers was carried out and summarized over area-averaging domains using the nine National Climatic Data Center (NCDC) climate regions (Figure 1c) [*Karl and Koss*, 1984]. Monthly and seasonal METDATA ET_0 anomalies were computed relative to the 1982–2009 monthly and seasonal climatology. Following the recommendation of *Kumar et al.* [2014], monthly CFSRF ET_0 anomalies were calculated relative to the CFSRF monthly climatology (1982–2009) from the corresponding initialization month and lead time. Season one forecasts are defined as the accumulated anomaly over the first 3 months after the initialization month (e.g., season one January–March (JFM) forecasts are initialized in December and represent the accumulated anomaly over JFM).

To assess skill of CFSRF, temporal anomaly correlations (AC) [*Miyakoda et al.*, 1972, equation 11] between CFSRF ensemble mean ET_0 and METDATA ET_0 were computed at monthly 1–9 month leads, and the season one forecasts (skill of ET_0 drivers is provided in the supporting information). ACs were computed for each grid point through time and then spatially averaged over each climate region. Skill during individual drought events was assessed based on the probability forecasts using the categorical Heidke skill score (HSS) [*O'Lenic et al.*, 2008; *Peng et al.*, 2013] (see supporting information for details). Drought events were defined based on METDATA when seasonal anomalies indicated that at least 50% of the regional area is above the eightieth percentile for ET_0 and below the twentieth percentile for Prcp (though not necessarily identical grid points).

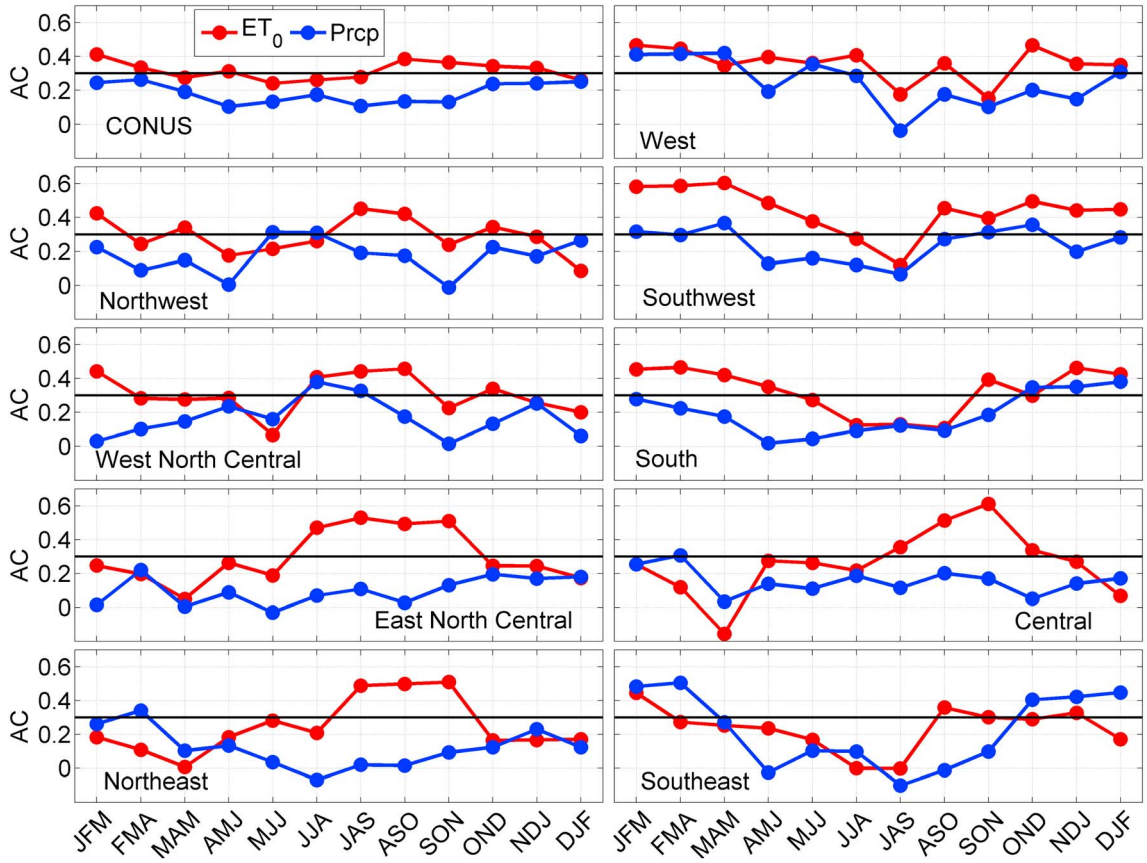

Figure 3. Season one anomaly correlation area-averaged over CONUS and individual climate regions. The black reference line indicates an anomaly correlation of 0.3, which represents the start of moderate skill according to the CPC.

This excludes events where ET_0 and Prcp show contrasting drought signals. Percentile thresholds were chosen based on the U.S. Drought Monitor classification scheme for moderate drought. For each drought event a spatial HSS was calculated using all grid points for each climate region.

3. Results

3.1. Deterministic Skill

Figure 2 shows spatially averaged monthly AC for ET_0 (Figures 2f–2j and 2p–2t) and Prcp (Figures 2a–2e and 2k–2o) over CONUS and its constituent NCDC climate regions. The National Oceanic and Atmospheric Administration's (NOAA) CPC currently uses an AC value of 0.3 as the threshold for a skill mask (AC $<$ 0.3 being considered to have no skill) in the real time CFSv2 forecasts. Maximum ET_0 AC for each region ranged from 0.41 (southeast; Figure 2t) to 0.66 (west; Figure 2q). Moderate skill (AC = 0.3 to 0.6) in ET_0 was maintained for important late winter and early growing season months of January through May for the southwest, south, and west at 1–5 month lead times (Figures 2r, 2s, and 2q, respectively) and for important late growing season and harvest period months of July through September for the east north central, central, and northeast at 1–3 months (Figures 2h, 2i, and 2j, respectively). For these same regions, months, and lead time ranges, consistent Prcp skill was absent. The west, southwest, and south regions all show a similar pattern of a sharp decline in ET_0 skill for target months of July through December. For Prcp skill a similar yet less congruent and weaker skill pattern is evident over the west and southwest regions, where enhanced Prcp predictability stems from initial conditions of ENSO region sea surface temperatures (SSTs) [e.g., *Wood et al.*, 2005; *Yuan et al.*, 2013]. This suggests that ET_0 predictability in these regions may also be related to SST initial conditions from the ENSO region in the late-summer and fall months, a hypothesis we examine further in subsequent sections.

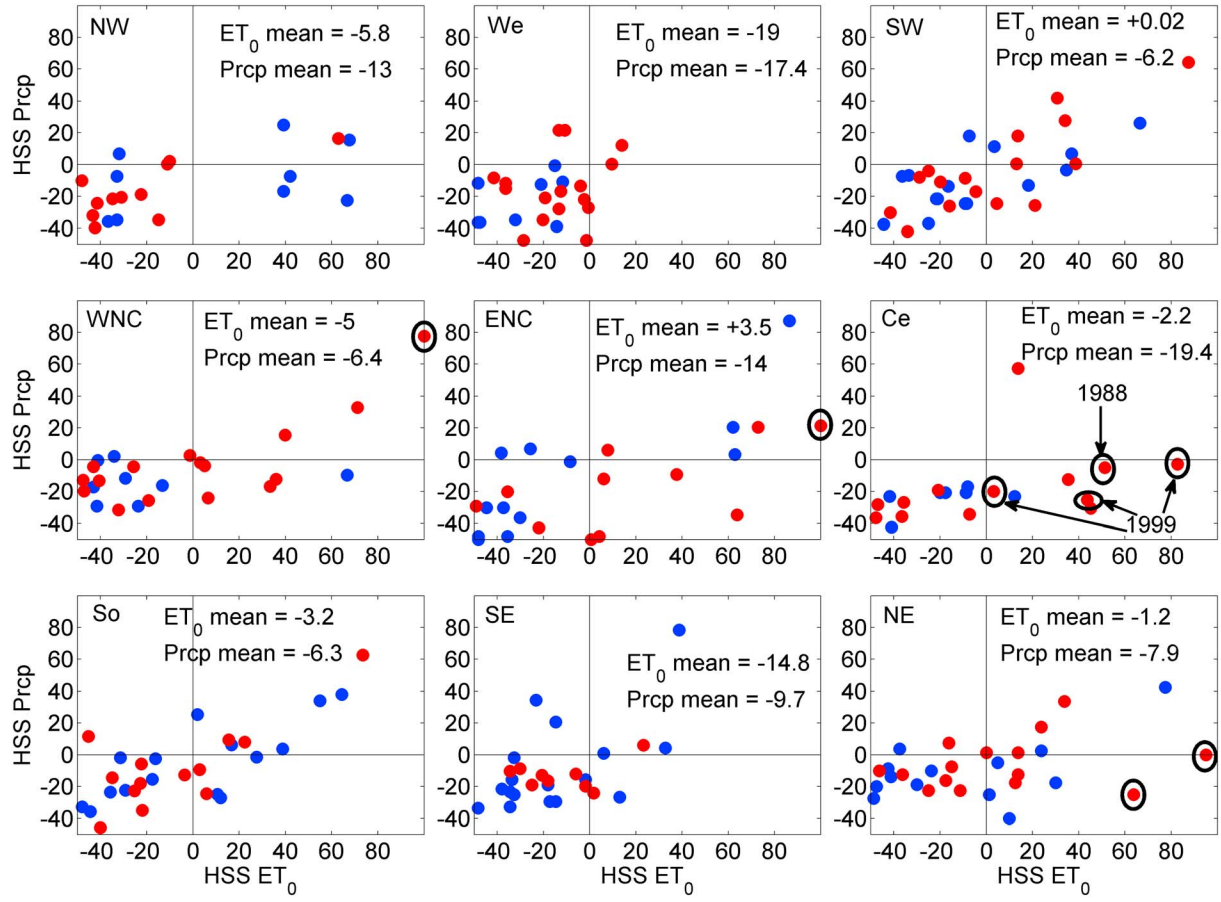

Figure 4. The HSS for season one forecasts for cases when both ET_0 and Prcp indicate drought (>80th percentile for ET_0 and <20th percentile for Prcp). Labels inside of each panel indicate region and mean HSS. Black circles show notable drought events of JJA 1988 in the WNC, ENC, and Ce, January–September (JAS), August–October (ASO), and September–November (SON) 1999 in the Ce, and May–July (MJJ) and JJA 1999 in the NE. These events are described in detail in the text. Red dots are for warm seasons (AMJ, MJJ, JJA, JAS, ASO, and SON) and blue dots are for cold seasons (October–December, November–January, DJF, JFM, February–April, and March–May).

In decomposing ET_0 drivers of T_{max}, T_{min}, R_d, and q, it was found that ET_0 skill is mostly a result of skill in T_{max} (Figure S2), T_{min} (Figure S3), and q (Figure S4). For some regions, such as the southwest, ET_0 and q actually have greater skill than T_{max} and T_{min} at times, which supports the conclusion that T_{air} is not always the dominant driver of ET_0 variability [*Hobbins*, 2016]. In regions and months when R_d (southeast region) and U_z (southwest and west regions) are the dominant drivers of ET_0 variability [*Hobbins*, 2016], poor skill in monthly forecasts of R_d and U_z (Figures S5 and S6 for, respectively) is likely adding to degraded overall ET_0 skill.

A more seasonal focused comparison of ET_0 and Prcp skill is provided below that highlights pertinent information on where and when ET_0 can add value to seasonal drought forecasts. Figure 3 illustrates season one AC for both ET_0 and Prcp averaged over CONUS and the nine U.S. climate regions. CONUS-wide, ET_0 skill is greater than Prcp during all seasons and remains above the 0.3 AC moderate skill threshold for more than half of the year. Most regions contain at least one or two seasons when ET_0 skill is much greater than Prcp (AC differences [$AC_{ET0} - AC_{Prcp}$] of ~0.2 to 0.5). Of particular interest are regions where ET_0 skill is high compared to Prcp skill during the growing season, such as in the east north central, central, and northeast regions, where enhanced reliability in seasonal drought forecasts could greatly benefit agricultural operations during mid and late season crop harvest periods. A second area of interest is in the southwest region, where moderate ET_0 skill during the fall, winter, and spring can result in improved water supply outlooks.

3.2. Categorical Skill of Probability Forecasts During Drought Events

Figure 4 illustrates region specific scatter plots of season one ET_0 HSS (*x* axis) and Prcp HSS (*y* axis) during drought events. Overall, two regions (southwest and east north central) were found to have positive (skillful)

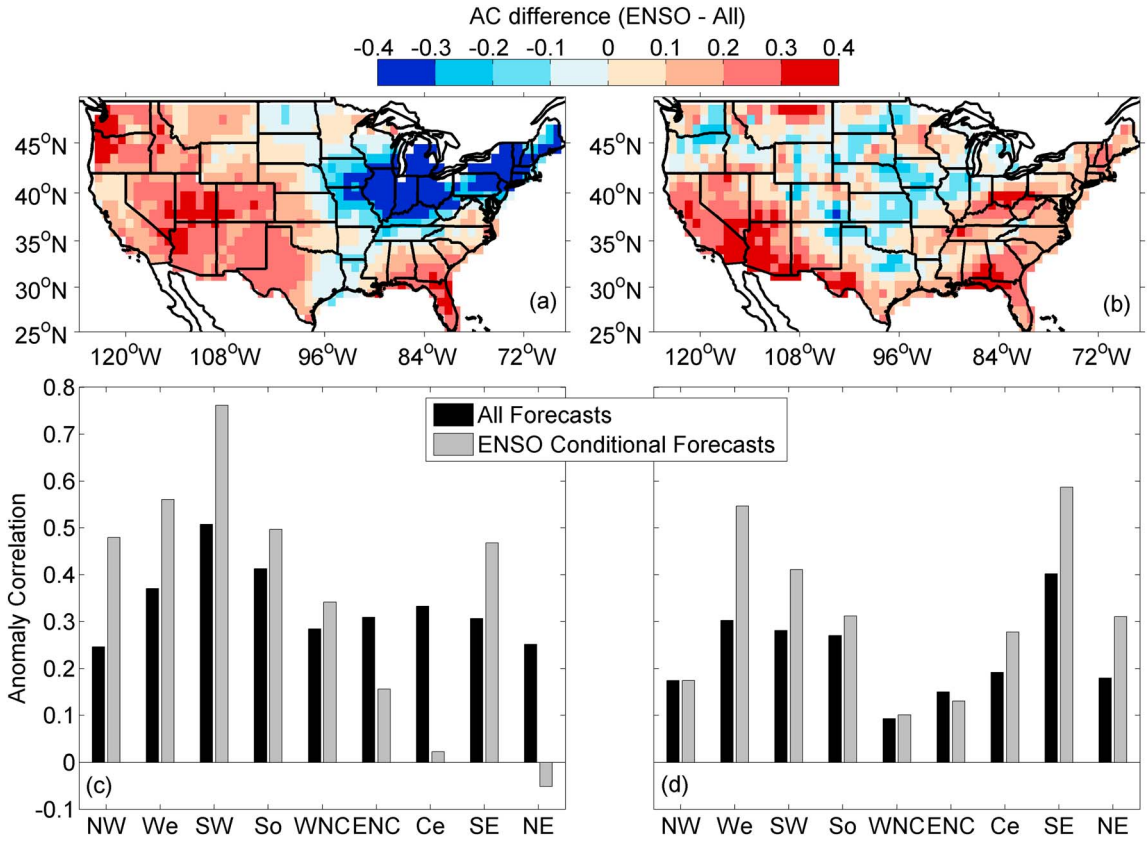

Figure 5. The difference in AC (fall-winter ENSO conditional forecasts minus all fall-winter forecasts) and regionally averaged AC for (a and c) ET_0 and (b and d) Prcp forecasts.

mean HSS using ET_0, while no regions were found to have positive mean HSS using Prcp. Although the mean HSS across all season one ET_0 forecasts was not skillful for most regions, many notable drought events were forecast skillfully with ET_0 and not with Prcp, as seen in the lower right ET_0 only skill quadrant of Figure 4 (quadrants defined by black reference lines) where there are more than double the number of events than the upper left Prcp only skill quadrant (38 and 15 total events in all regions for the lower right and upper left quadrants, respectively). Drought events, such as the summer (June–August (JJA)) of 1988, one of the worst droughts in the Central U.S. since the infamous "dust bowl," were forecast well using both ET_0 and Prcp in the west north central and east north central regions. However, positive skill was only found with ET_0 in the central region. Another event that was forecast well with ET_0 and where Prcp skill was poor was the summer and fall of 1999, a drought event that had devastating impacts on the central and northeast regions. The aforementioned drought events are annotated in Figure 4. These results illustrate that ET_0 forecasts generally have higher skill than Prcp forecasts for predicting drought events.

3.3. ENSO as a Source of Predictability

Seasonal forecast skill of T_{air} and Prcp over CONUS, and ET_0 over a portion of the southeast region, have been found to increase when CFSRF and global spectral model (predecessor to CFS) forecasts are initialized during moderate and strong ENSO events [*Wood et al.*, 2005; *Yuan et al.*, 2013; *Tian et al.*, 2014]. To investigate ENSO as a source of ET_0 predictability over CONUS, all season one forecasts were compared against ENSO conditional forecasts defined as when the Oceanic Niño Index (ONI) from the CPC (http://www.cpc.ncep.noaa.gov/products/analysis_monitoring/ensostuff/ensoyears.shtml) exceeds ±1°C. ONI is one of several ENSO indices and results could vary depending on choice of index [e.g., *Capotondi et al.*, 2015]. Only forecasts initialized during ENSO events were considered and not the month for which the forecast was made. A total of 76 ENSO conditional initialization months were classified during the period of record out of 336 possible season one forecasts and 52 out of 76 ENSO initial months occurred in fall-winter (September through February).

Results are only shown for fall-winter; the seasons when ENSO has the greatest impacts on CONUS. Temporal AC was computed over each grid point for fall-winter ENSO conditional and all fall-winter season one forecasts and then spatially averaged over each climate region. A caveat to this approach is that forecasts may not be completely independent of each other (e.g., a forecast made in November for December-February (DJF) and one made in December for JFM rely on independent atmospheric initial conditions but ENSO region SSTs may be similar) which may reduce the degrees of freedom in a given sample.

Figure 5 shows the difference in AC between fall-winter ENSO conditional initial months and all fall-winter forecasts using ET_0 (Figure 5a) and Prcp (Figure 5b). Spatial patterns of forecast improvement (positive AC differences) are quite similar for both ET_0 and Prcp over parts of the west, southwest, south and southeast regions. Improvements in forecast skill of Prcp are consistent with previous research in the west, southeast, and southwest regions [e.g., *Wood et al*., 2005; *Yuan et al*., 2013] and are consistent with *Tian et al*. [2014] over the southeast region for ET_0. Spatial patters of ET_0 and Prcp AC difference are contrasting in much of the northern half of CONUS, where ET_0 forecasts are greatly improved in the northwest region, while Prcp forecasts are improved in the northeast and central regions. ENSO teleconnection are generally weaker in the regions where skill ET_0 gets lower (e.g., the northeast and central), but it has yet to be concluded that this is the reason for degraded forecast skill. Overall, ET_0 skill is considerably higher than Prcp during ENSO conditional forecasts (Figures 5c and 5d). This is particularly evident in the northwest and southwest regions, with similar skill found in the west and southeast regions, and only minor changes in skill were found in the south, west north central, and east north central regions.

4. Discussion and Conclusions

This study highlights a novel CONUS-wide assessment of seasonal ET_0 forecast anomalies using CFSRF and METDATA observations. Nine climate regions were used as area-averaging domains to assess regional skill variability. Monthly ensemble mean forecasts were analyzed at leads of 1–9 months, and season one ensemble mean forecasts were used to highlight seasonal skill variability. Monthly ET_0 ACs revealed large regional and seasonal variability, with moderate skill (AC of 0.3–0.6) found at leads of 1–5 months and no consistent skill at longer lead times.

Seasonal ET_0 skill was found to be consistently greater than Prcp skill when averaged over CONUS, and the same is true for most regions where large AC differences (0.2–0.5) were found depending on season. Assessment of probability forecasts during drought events using the HSS revealed high skill in ET_0 for some regions and seasons, particularly over the southwest and east north central regions. Two of the most severe droughts during the period of record (summer of 1988 and summer-fall of 1999) were forecast with reasonable skill using ET_0 and with poor skill using Prcp. While it is still unclear what makes certain drought events more predictable than others, one prominent feature during 1988 and 1999 (northeast only) was high T_{air}, which likely improved ET_0 over Prcp forecasts. Another interesting finding is that poor Prcp forecasts are not always coincident with poor ET_0 forecasts, which potentially indicates a lack of land surface-atmospheric coupling in CFSv2 for certain drought events. Findings from ET_0 and Prcp skill analyses indicate that including ET_0 anomalies in operational seasonal drought forecasts would provide additional skill and confidence for various applications such as agricultural and water resource outlooks throughout CONUS.

Results illustrating the skill of ENSO conditional versus all events show that some portion of ET_0 predictability comes from the initial state of tropical Pacific SSTs. This is evident from similar skill patterns found between ET_0 and Prcp in the west, southwest, and southeast regions (Figures 2 and 5), where several studies have found enhanced Prcp and T_{air} skill during strong ENSO events [e.g., *Wood et al*., 2005; *Yuan et al*., 2013]. *Tian et al*. [2014] also found enhanced ET_0 predictability in the southeast during the cold season when CFSv2 forecasts were initialized during ENSO events. *Jia et al*. [2015] found seasonal Prcp skill from the Geophysical Fluid Dynamics Laboratory climate model to be mostly ENSO related, but T_{air} skill to be related to ENSO in addition to a multidecadal warming signal, which could be an additional factor contributing to ET_0 skill from CFSv2. *Peng et al*. [2013] also found that the warming trend in CFSv2 enhanced categorical T_{air} forecast skill (when compared to CFSv1) due to the addition of a time-evolving carbon dioxide concentration not used in CFSv1. Initial state of the soil moisture column could also be contributing to ET_0 predictability considering energy balance feedbacks between the land and near surface boundary layer, thus affecting variables

of T_{max}, T_{min}, and q used to generate ET_0 estimates. *Yoon and Leung* [2015] found antecedent soil moisture to be as important as ENSO in seasonal Prcp forecast skill over parts of CONUS, and given the high correspondence in ET_0 and Prcp anomalies (Figures 1 and S1), it is expected that soil moisture would be another source of predictability for ET_0 forecasts.

Skillful seasonal climate predictions remain a major challenge in drought forecasting; however, the use of ET_0 anomalies from CFSv2 clearly show improvements over Prcp forecasts over most regions and seasons and can improve and complement existing seasonal drought forecasts. Further research and skill improvements are needed for reliable operational use of ET_0 (and other metrics) in seasonal drought forecasting. Identifying why certain droughts are more predictable than others is a research area that would greatly benefit operational seasonal drought forecasting.

Acknowledgments
Daniel McEvoy, John Mejia, and Justin Huntington were all partially supported by the Desert Research Institute (DRI) IBM PureSystems, Institute Project Assignments-Enhanced Seasonal Forecasts for Western United States, Bureau of Reclamation Climate Analysis Tools WaterSMART program (Public Law 111-11, Section 9504(b), agreement R11AP81454), and the National Integrated Drought Information System (NIDIS). Michael Hobbins acknowledges support from Inter-Agency Agreement AID-FFP-P-10-00002/006 between USAID and NOAA for their support to the Famine Early Warning Systems Network. Links to METDATA and CFSRF used in this study can be found in the references.

References

Abatzoglou, J. T. (2011), Development of gridded surface meteorological data for ecological applications and modeling, *Int. J. Climatol.*, *33*, 121–131, doi:10.1002/joc.3413. [Available at http://nimbus.cos.uidaho.edu/DATA/OBS/.]

Allen, R. G., I. A. Walter, R. Elliott, T. Howell, D. Itenfisu, and M. Jensen (2005), The ASCE standardized reference evapotranspiration equation, *Rep*. 0-7844-0805-X, 59 pp. [Available at http://www.kimberly.uidaho.edu/water/asceewri/ascestzdetmain2005.pdf.]

Anderson, M. C., C. R. Hain, B. Wardlow, J. R. Mecikalski, and W. P. Kustas (2011), Evaluation of a drought index based on thermal remote sensing of evapotranspiration over the continental United States, *J. Clim.*, *24*, 2025–2044, doi:10.1175/2010JCLI3812.1.

Capotondi, A., et al. (2015), Understanding ENSO Diversity, *Bull. Am. Meteorol. Soc.*, *96*, 921–938, doi:10.1175/BAMS-D-13-00117.1.

Daly, C., R. P. Neilson, and D. L. Phillips (1994), A statistical-topographic model for mapping climatological precipitation over mountainous terrain, *J. Appl. Meteorol.*, *33*, 140–158.

Dirmeyer, P. A. (2013), Characteristics of the water cycle and land-atmosphere interactions from a comprehensive reforecast and reanalysis, *Clim. Dyn.*, *41*, 1083–1097, doi:10.1007/s00382-013-1866-x.

Hobbins, M. T. (2016), The variability of ASCE standardized reference evapotranspiration: A rigorous, CONUS-wide decomposition and attribution, *Trans. ASABE*, *59*, doi:10.13031/trans.5910975, in press.

Hobbins, M. T., and J. L. Huntington (2016), Chapter 42, in *Handbook of Applied Hydrology*, edited by V. P. Singh, McGraw-Hill Education, New York.

Hobbins, M. T., A. Dai, M. L. Roderick, and G. D. Farquhar (2008), Revisiting the parameterization of potential evaporation as a driver of long-term water balance trends, *Geophys. Res. Lett.*, *35*, L12403, doi:10.1029/2008GL033840.

Jia, L., et al. (2015), Improved seasonal prediction of temperature and precipitation over land in a high-resolution GFDL climate model, *J. Clim.*, *28*, 2044–2062, doi:10.1175/JCLI-D-14-00112.1.

Karl, T. R., and W. J. Koss (1984), *Regional and National Monthly, Seasonal, and Annual Temperature Weighted by Area, 1895–1983*, *Hist. Climatol. Ser.*, vol. 4–3, 38 pp., Natl. Clim. Data Cent., Asheville, N. C.

Kumar, S., P. A. Dirmeyer, and J. L. Kinter III (2014), Usefulness of ensemble forecasts from NCEP Climate Forecast System in sub-seasonal to intra-annual forecasting, *Geophys. Res. Lett.*, *41*, 3586–3593, doi:10.1002/2014GL059586.

Lavers, D., L. Luo, and E. F. Wood (2009), A multiple model assessment of seasonal climate forecast skill for applications, *Geophys. Res. Lett.*, *36*, L23711, doi:10.1029/2009GL041365.

McEvoy, D. J. (2015), Physically based evaporative demand as a drought metric: Historical analysis and seasonal prediction, PhD dissertation, Dep. of Atmospheric Science, Univ. of Nevada, Reno, Nevada. [Available online at http://www.dri.edu/images/stories/divisions/das/dasfaculty/mcevoy_dissertation_final.pdf.]

Mitchell, K. E., et al. (2004), The multi-institution North American Land Data Assimilation System (NLDAS): Utilizing multiple GCIP products and partners in a continental distributed hydrological modeling system, *J. Geophys. Res.*, *109*, D07S90, doi:10.1029/2003JD003823.

Miyakoda, K., G. D. Hembree, R. F. Strickler, and I. Shulman (1972), Cumulative results of extended forecast experiments: I. Model performance for winter cases, *Mon. Weather Rev.*, *100*, 836–855, doi:10.1175/1520-0493(1972)100<0836:CROEFE>2.3.CO;2.

Mu, Q., M. Zhao, J. S. Kimball, N. G. McDowell, and S. W. Running (2013), A remotely sensed global terrestrial drought severity index, *Bull. Am. Meteorol. Soc.*, *94*, 93–98, doi:10.1175/BAMS-D-11-00213.1.

O'lenic, E. A., D. A. Unger, M. S. Halpert, and K. S. Pelman (2008), Developments in operational long-range climate prediction at CPC, *Weather Forecasting*, *23*, 496–515, doi:10.1175/2007WAF2007042.1.

Otkin, J. A., M. C. Anderson, C. Hain, I. E. Mladenova, J. B. Basara, and M. Svoboda (2013), Examining rapid onset drought development using the thermal infrared–based evaporative stress index, *J. Hydrometeorol.*, *14*, 1057–1074, doi:10.1175/JHM-D-12-0144.1.

Peng, P., A. G. Barnston, and A. Kumar (2013), A comparison of skill between two versions of the NCEP Climate Forecast System (CFS) and CPC's operational short-lead seasonal outlooks, *Weather Forecasting*, *28*, 445–462, doi:10.1175/WAF-D-12-00057.1.

Saha, S., et al. (2014), The NCEP Climate Forecast System Version 2, *J. Clim.*, *27*, 2185–2208, doi:10.1175/JCLI-D-12-00823.1. [Available at http://nomads.ncdc.noaa.gov/data/cfsr-rfl-mmts/.]

Shukla, S., M. Safeeq, A. AghaKouchak, K. Guan, and C. Funk (2015), Temperature impacts on the water year 2014 drought in California, *Geophys. Res. Lett.*, *42*, doi:10.1002/2015GL063666.

Tian, D., C. J. Martinez, and W. D. Graham (2014), Seasonal prediction of regional reference evapotranspiration based on Climate Forecast System Version 2, *J. Hydrometeorol.*, *15*, 1166–1188, doi:10.1175/JHM-D-13-087.1.

Weiss, J. L., C. L. Castro, and J. T. Overpeck (2009), Distinguishing pronounced droughts in the southwestern United States: Seasonality and effects of warmer temperature, *J. Clim.*, *22*, 5918–5932, doi:10.1175/2009JCLI2905.1.

Williams, A. P., R. Seager, J. T. Abatzoglou, B. I. Cook, J. E. Smerdon, and E. R. Cook (2015), Contribution of anthropogenic warming to California drought during 2012–2014, *Geophys. Res. Lett.*, *42*, 6819–6828, doi:10.1002/2015GL064924.

Wood, A. W., A. Kumar, and D. P. Lettenmaier (2005), A retrospective assessment of National Centers for Environmental Prediction climate model–based ensemble hydrologic forecasting in the western United States, *J. Geophys. Res.*, *110*, D04105, doi:10.1029/2004JD004508.

Wood, E., S. Schubert, A. Wood, C. Peters-Lidard, K. Mo, A. Mariotti, and R. Pulwarty (2015), Prospects for advancing drought understanding, monitoring and prediction, *J. Hydrometeorol.*, *16*, 1636–1657, doi:10.1175/JHM-D-14-0164.1.

Yao, Y., S. Liang, Q. Qin, and K. Wang (2010), Monitoring drought over the conterminous United States using MODIS and NCEP reanalysis-2 data, *J. Appl. Meteorol. Climatol.*, *49*, 1665–1680, doi:10.1175/2010JAMC2328.1.

Yoon, J., and L. R. Leung (2015), Assessing the relative influence of surface soil moisture and ENSO SST on precipitation predictability over the contiguous United States, *Geophys. Res. Lett.*, 5005–5013, doi:10.1002/2015GL064139.

Yuan, X., E. F. Wood, L. Luo, and M. Pan (2011), A first look at Climate Forecast System version 2 (CFSv2) for hydrological seasonal prediction, *Geophys. Res. Lett.*, *38*, L13402, doi:10.1029/2011GL047792.

Yuan, X., E. F. Wood, J. K. Roundy, and M. Pan (2013), CFSv2-based seasonal hydroclimatic forecasts over the conterminous United States, *J. Hydrometeorol.*, *26*, 4828–4847, doi:10.1175/JCLI-D-12-00683.1.